Proceedings of the IASS 2024 Symposium
Redefining the Art of Structural Design
August 26-30, 2024, Zurich, Switzerland
Philippe Block, Giulia Boller, Catherine DeWolf,
Jacqueline Pauli, Walter Kaufmann (eds.)

Envelope Optimization: Shape- and Thickness-Optimization for multiple Load Cases

Patrick SCHÄFERLING*, Matthias BECKH*

* Technical University Dresden
Faculty of Architecture, Chair of Structural Design
Zellescher Weg 17, 01069 Dresden
patrick.schaeferling@tu-dresden.de

Abstract

The optimization of shell structures remains a subject of extensive research. When considering variable loads, existing models and methods reach their limitations. Due to the complex interdependencies and interactions of multi load case scenarios, form-finding for compression-only shells often focuses solely on self-weight and constant loads. The dimensioning of the cross section usually takes place after the form-finding, to accommodate all relevant load cases. This paper presents a first investigation of an integrated shape- and thickness-optimization for multi load-case scenarios.

The basic idea is an alternative formulation of the spring elements in the particle-based simulation. The direction of force remains collinear to the spring direction to ensure compression-only elements. However, the exerted spring force is no longer calculated from the element's individual elongation. This adaptation allows the manipulation of the force flow within the structure while preventing horizontal displacement of the particles. Limiting the particle's degrees of freedom facilitates to adjust the load cases' individual thrust-lines, to effectively reduce the enveloping cross section.

The paper describes the fundamental concept, mechanism, and the first digital exploration. The individual steps are illustrated using an exemplary 2D arch structure. The research holds potential of increasing the efficiency of structures significantly. It can eliminate the necessity for the constant loads to be the sole decisive load in shape-optimization, opening up a wide field of new application scenarios. Consequently, comparatively lightweight but compression-resistant materials may also become appealing for compression-only structures.

Keywords: Form-finding, Multi-Objective Optimization, Multi Load-Cases, Variable Loads, Cross Section Optimization, Envelope Optimization

1. Introduction

Form finding for compression only structures can dramatically reduce material consumption, consequently mitigating the environmental impact of the designed structures. The roots of numerical form finding methods can be traced back to the 1960s, when the transition from physical models to the initial stages of digital simulation marked a pivotal moment in the field. Numerical simulations, at their inception, sought to emulate the behaviors observed in physical models, laying the groundwork for today's frameworks. Driven by the increased computational power in the 1990s, methodological advancements were setting the stage for a new era in structural optimization. The ability to digitally simulate and optimize structures opened avenues for more efficient and sustainable design practices.

An overarching characteristic of most form finding methods is their focus on one dominating load case. This practice relates to the exponentially growing complexity of additionally constrained systems. However, it introduces a limitation that echoes through the entire design process. The simplified models restrict the applicability of the optimization method to a narrow spectrum of construction methods and materials, like concrete or stone, because only they bring the recommended specific weight for a dominating self-weight load-case. With the possibility to integrate various load case scenarios in the optimization procedure, the dead load must not be the dominant load anymore. Hence, more construction materials, including unconventional choices like foam glass or wood seem promising for compression only structures. In response to this challenge, the paper presents a first investigation of simultaneous multi-load-case shape and cross section optimization based on a dynamic, particle-based simulation. It allows for a bottom-up approach and holds the potential for further extension.

2. Thrust lines and cross sections for multiple load cases

The lower bound theorem for masonry, as formulated by Jaques Heymann [1], states that an unreinforced structure remains safe under specific loads, as long as there exists at least one compressive solution that equilibrates them, forming a thrust line (TL) that fits within the structure's cross section, as shown in Figure 1.

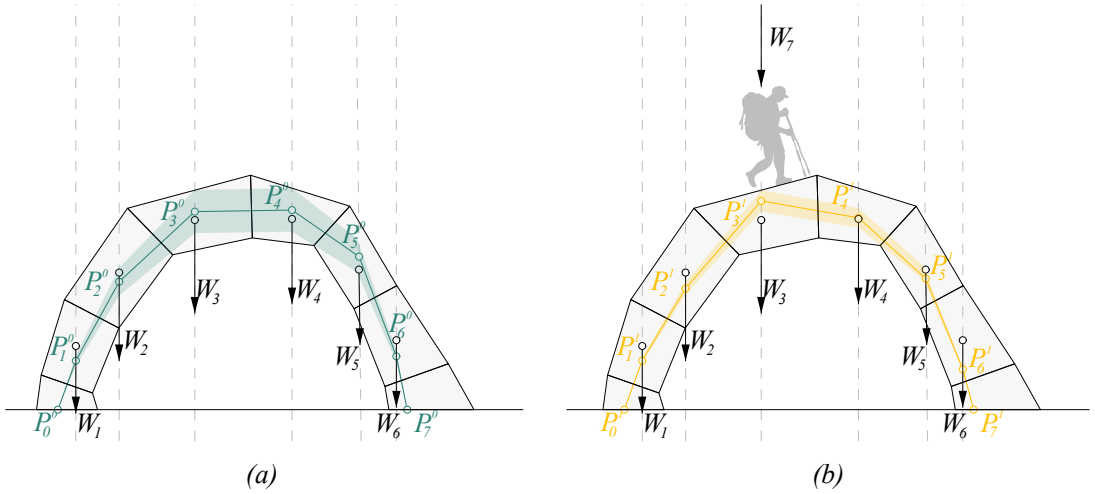

Figure 1: Thrust-lines for two different load-cases: (a) dead load and (b) dead load + point load, with corresponding solution spaces (possible scaling) for each individual thrust-line in the given cross section.

The historical strategy to reinforce such compression only structures for asymmetric loading, used until today, is to globally increase the cross sectional area. This strategy yields a doubly stabilizing effect for asymmetric load cases. On the one hand, a larger cross section results in higher mass of the structure. Since the shape of the TL emerges from the equilibrium of all applied loads, the influence and therefore the displacement of the asymmetric loaded TLs (in relation to the TL of solely dead load) gets reduced. On the other hand, an increased cross section provides more space to accommodate thrust lines of asymmetric load scenarios [2]. However, this approach brings some mayor disadvantages. Firstly, material choice gets narrowed down dramatically as this strategy is only effective with materials of high specific weight. Moreover, globally increasing the cross section, and thereby the overall material consumption, does not align with the goal of reducing the environmental impact by form finding and optimization. This particularly holds true when dealing with modern high-tech materials with high environmental im-

pact like (UHP-) concrete. By extending the form finding procedure for compression-only structures to multiple load cases, the necessary cross section can theoretically be reduced to the minimum required dimension. Minimum in this case means the one cross section, which still respects the lower bound theorem for masonry for all simulated load cases. With this strategy unnecessary material usage and environmental impact can be minimized, while maintaining a pure compression state in all load cases. However, this leads to some challenging problems which are briefly explained in the following subsections.

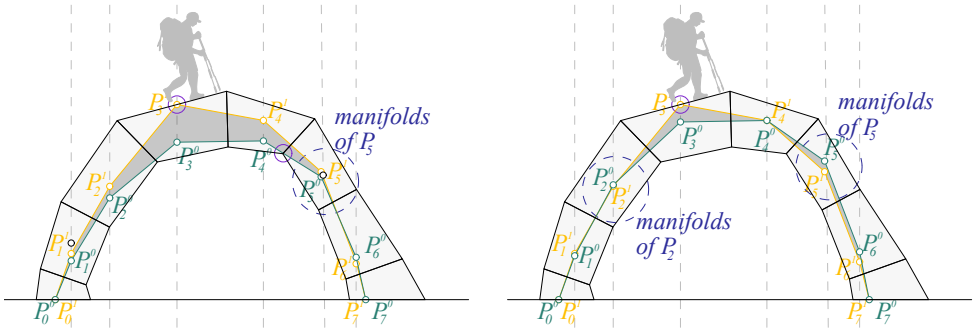

Figure 2: Problem with individual scaling: two versions of thrust-lines with different scaling and corresponding envelope cross section (dark gray). The dead load will be determined by the cross section in the next iteration.

2.1. Increased complexity of the iterative calculation

The core of form finding is to determine the shape of the TL under given loads. In the simulation of dynamic particle based methods (choice of solver method see section 3.) the TL is represented by a discretized curve (polyline), which is defined by control points as shown in Figure 1. Loads are accumulated to "lumped masses" and applied to the control points of the polyline. Extending the method to multi load case scenarios, each TL and therefore each control point is represented by manifolds for every single load case, shown in Figure 2. This extension is increasing the total number of nodes n in the simulation to $n\ lc$, where lc is the total number of load cases.

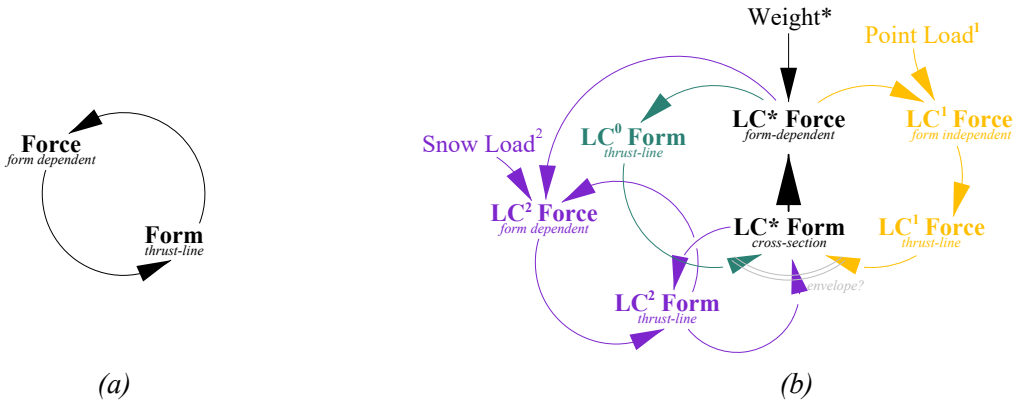

Figure 3: Increasing complexity when adding load cases to the form finding.

Following the lower bound theorem for masonry, each TL manifold has to fit within the global cross section. However, the cross section itself is defined by the very same TLs. The increasing interdepen-

dencies with additional load-cases is shown in Figure 3b for an additional point load (form-independent) and snow load (form-dependent, like the dead load). These additional interdependencies increase the load-case related constraints of each node from lc to $(lc^2 - 1)$. Solving for these constraints significantly increases the complexity of the calculation and requires fast algorithms to handle the increasing number of constraints.

2.2. Stability of the solver

Increasing numbers, contradicting or non-continuous constraints decrease the stability of the problem. The enveloping cross section for example, is a non-continuous constraint as the cross section is defined by only two (upper and lower limit) of all control point manifolds, which can change suddenly from iteration to iteration. The method has to provide sufficient stability to handle such discrete constraints.

2.3. Bending moments from varying horizontal displacement

Varying horizontal displacement of the control point's manifolds leads to varying mass accumulation in different load cases. This can introduce bending moments, potentially compromising structural integrity as shown in Figure 4. The most critical regions for this problem are the perimeters of the shell, when thrust-surfaces of variable loads exceed the horizontal area of the constant load case.

2.4. Determination of the envelope cross section

Under most circumstances it is very difficult to determine which of the points' manifolds actually has to delineate the cross section. While some particles may have a lower z-coordinate than their manifolds, they can nevertheless be the upward limiting entity due to horizontal displacement as shown in Figure 4. This problem gets even more complex in 3D-space. It could be solved geometrically - creating the actual TL geometry (thrust surface in 3D) from the control points, projecting the manifold particles onto the geometry and analyzing the projection vector. The problem with this strategy is the computational cost, because it has to take place every iteration.

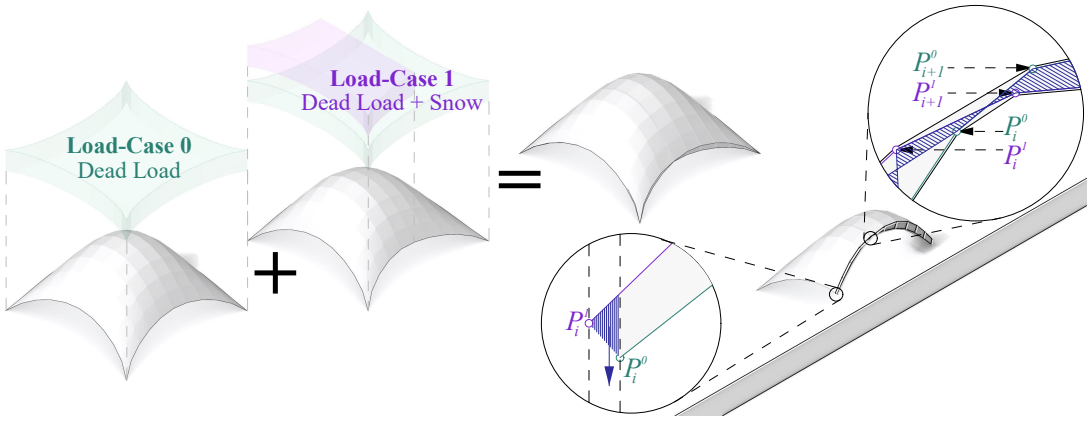

Figure 4: Problems with bending and determination of the envelope.

In summary, while the lower bound theorem provides a theoretical framework for ensuring the safety of masonry structures under specific load conditions, its extension to multiple load cases introduces complexities that must be addressed carefully. Tackling issues such as load case interdependencies and the accumulation of lumped masses requires both advanced computational techniques and refined formulation strategies to ensure the structural integrity and efficiency of the optimized designs.

3. The solver method

Veenendaal and Block [3] categorized computational form finding methods in 3 main groups: stiffness matrix methods, geometric stiffness methods and dynamic equilibrium methods. As we are tackling problems with a large number of nodes and constraints as described in section 2., the total operation count and stability are the main parameters to choose the calculation method. However we still want to use a true inverse form finding method (finding the exact solution) according to the categorization of Cuvilliers [4]. For our purpose and state of knowledge, dynamic particle based methods have some decisive advantages in these fields.

Most important, all required terms in the element's strain-displacement or force-displacement relations can be considered in the initial formulation of the constraints, and the corresponding internal force vector can easily be derived. There is no need for (higher-order) derivative calculation in the iterative procedure, thus simplifying the mathematics [5]. Especially the low level mathematical formulation is very important for the exploration of a design oriented optimization method that is used and extended by users of various professions. Also, in particle based methods the solution is obtained by recursive procedure, so only a few lines of code is required compared to equation solvers for NR-type methods[6]. This facilitates the possibility of later-on-extension with respectively low effort, like adding manufacturing related constraints to the form finding.

The most known dynamic equilibrium methods in the field of structural design are supposedly Dynamic Relaxation (DR) [7] and Particle Spring Systems (PS) [8]. However, with the recent trend in Artificial Intelligence (AI), Machine Learning (ML) and applied statistics, huge steps were made in computational methods for distributed minimization algorithms, tackling stability problems as well as speed and efficiency. This led to a new generation of particle based solvers, mostly in the field of computer game engines, which can also be used for form finding. The Alternating Direction Method of Multipliers (ADMM)[9], Projective Dynamics Method (PDM) [10] or Constraint Projection Method (PCM) [11] are simple but powerful algorithms that are well suited to distributed convex optimization, in which the large optimization problems are decomposed to small local sub-problems and coordinated to find a global solution. By using augmented lagrangians, ADMM is very robust. It is suited for very stiff problems (high impact of the constraint to reach the projected horizontal origin) see subsection 4.1., as well as problems which are not strictly convex or finite, like the envelope cross section constraints [9]. Therefore we chose to do the first steps with the Kangaroo 2 Solver, which builds on ideas of ADMM and PDM and gives the possibility to design custom goal objects for the calculation [12]. The solver is sufficient for simple examinations of multi load-case form finding with reduced number of nodes and load-cases. There is no possibility to build manifolds of nodes, why we used the y-direction to 'layer' manifolds in space for this paper. To increase speed and enable dimension-independent manifolds, a specific solver or implementation is the desired next step of this project.

4. Simulation Elements

In the following subsections, the constraints of the conducted simulations are described. They can be determined separately because of the chosen solver method. This splits the problem statement in separate steps.

4.1. Projection-Oriented Spring

As described in subsection 2.3. and subsection 2.4., horizontal displacement is a huge problem for multi load case form finding. Our strategy is to simply avoid the problem by limiting the horizontal displacements of the nodes' manifolds with the constraint definitions. This can be accomplished by an

alternated formulation of the spring elements.

There already has been some research in the definition of spring equations, limiting their end nodes to vertical movement during form finding. Harding and Shepherd [13] suggested the use of "zero-length springs" [14] in combination with dynamically updated lumped masses. The zero-length springs obey Hooke's Law, but have a natural length of 0, therefore the exerted force is directly proportional to the length of the spring. This can limit the horizontal displacements when two boundary conditions are fulfilled: firstly, all initial spring elements have to have the same length, which limits the topology and the shape of the structures quite dramatically; secondly, all boundary nodes have to be fixed (at least horizontally).

To not restrict the design freedom so drastically, we chose to limit the displacement of the nodes in a different manner. Starting from the vector form of Hook's Law in Equation (1), where p_0^0 and p_1^0 are the initial nodes of the spring elements, p_0^i and p_1^i their representations in the current iteration and k the spring constant, $1 - (|p_0^i - p_1^i|/|p_0^0 - p_1^0|)$ can be described as stretch factor, derived from the ratio of current to initial length. By adjusting this stretch factor one can manipulate the exerted force of the spring without compromising the aimed membrane state, the force direction is still determined by the actual spring direction.

$$\boldsymbol{f} = k\,(1 - \frac{|p_0^i - p_1^i|}{|p_0^0 - p_1^0|})(p_0^i - p_1^i) \tag{1}$$

Multiplying the individual coordinates of the stretch factor by a transformation matrix E_b, in this case for the xy-Plane, that is normal to the applied loads, leads to a stretch factor that reacts to the projected elongation instead of the actual one. On the element level this change only has minor influence on the elements behavior. However, in the global system, when all spring elements aim to reach their initial projected length, it leads to converging minimization of the nodes' displacement with respect to the projection plane.

$$E_b = \begin{pmatrix} 1 & 0 & 0 \\ 0 & 1 & 0 \\ 0 & 0 & 0 \end{pmatrix}, \quad \boldsymbol{f} = k\,(1 - \frac{|E_b \cdot (p_0^i - p_1^i)|}{|E_b \cdot (p_0^0 - p_1^0)|})(p_0^i - p_1^i) \tag{2}$$

Like the zero-length approach, the Projection-Oriented Spring (POS) comes at a cost. The projection is only congruent to the initial state of the network when non-collinear fixed points exist. Additionally, the initial configuration must obey the constraints for compression only structures analogously to the configuration of the 'primal grid' in the Thrust-Network Analysis (TNA) [15]. Unlike TNA, this must not be a failure criterion for the form finding, but if the primal grid does not meet all thrust-network related criteria, horizontal displacement will occur.

Lastly, the POS only reacts to displacement with respect to the projection plane. As the elements converge towards their initial projected length, the exerted force reduces to 0. Applied loads can not longer be equilibriated by the POS when converging. This behavior relates to the scalability of thrust-lines in the direction of the applied loads and there is an infinite number of scale factors for working configurations of a primal grid. By scaling the form one can directly control the horizontal forces in the system. In TNA the exact solution can only be computed from the dual grid with the additional definition of a scale factor, in the implementation RhinoVault2 [16] this is realized with a target height. This required, additional constraint could also be some other variable - like maximum normal force, maximum slope or any kind of cross section related constraint.

4.2. Self weight

Self weight is usually calculated by the tributary area of the nodes. With multiple load cases, the required cross section has to be determined with the lower bound theorem of masonry. With the use of POSs, node manifolds are aligned normal to the projection plane (here: z-direction). The required cross section can therefore directly be derived from the manifolds' envelope, the maximum and minimum z-coordinate. To ensure a minimum thickness of the cross section we add a constant parametric value to this minimal thickness.

4.3. Height constraints

As already mentioned in subsection 4.1. an additional constraint is needed to determine a specific solution in membrane state. We want to make use of this requirement and suggest constraints that align the different load case specific thrust lines individually to effectively reduce the required cross section.

The first approach is to define a global maximum height z^{max} of the individual TLs, as realized in RhinoVault2. The constraint definition is derived from the spring equation (1). The stretch factor and therefore the exerted spring force is calculated with a combined positivity constraint function $s(p^i_{0z}, p^i_{1z}, z_{max})$ for the z-coordinates of the nodes p^i_0 and p^i_1, the direction of the force remains unchanged. When exceeding the globally defined z-limit, the spring starts to exert force, leading to horizontal displacement in the first step. The horizontal movement will be equilibriated by the systems' POSs in the following iterations. Tests of this constraint show no correlation to cross sectional area, although it can be very efficient in some cases.

$$h(z_1, z_2) = \begin{cases} z_1 - z_2 & \text{if} \quad z_1 - z_2 \geq 0 \\ 0 & \text{if} \quad z_1 - z_2 < 0 \end{cases} \tag{3}$$

$$s(p^i_{1z}, p^i_{2z}, z_{max}) = h(p^i_{1z}, z_{max}) + h(p^i_{2z}, z_{max}) \tag{4}$$

$$F^{maxheight}_{P0} = k\ s(p^i_{0z}, p^i_{1z}, z_{max})(p^i_1 - p^i_0) = -F^{maxheight}_{P1} \tag{5}$$

The second approach uses the same calculation method as the first one [equation (5)], but an average height of the manifold points instead of a global value z_{max}. The manifold average z-value gets updated every iteration.

4.4. Slope constraints

The force in a catenary relates to the slope (in force direction), so our second approach for additional constraints, to minimize the cross section, is based on the slope of the POSs. The first attempt was to approach a globally defined slope. The stretch factor, and therefore the exerted force F^{gs} is directly derived from the nodes' coordinates, like shown in equation (6). The steeper, the larger the exerted force gets. Again, this initially leads to horizontal displacement, which will be equilibriated in the following iterations. Tests showed that this approach can reduce the global cross section by relating all TLs to a globally defined goal.

$$F^{gs}_{P0} = k\ (1 - \frac{|p^i_{1z} - p^i_{0z}|}{|p^i_1 - p^i_0|})\ (p^i_1 - p^i_0) = -F^{gs}_{P1} \tag{6}$$

$$v_{avg} = \frac{\sum_{i=0}^{lc-1} |p^i_1 - p^i_0|}{lc - 1}, \quad F^{as}_{P0} = k\ (1 - \frac{|p^i_{1z} - p^i_{0z}|}{v_{avg}})\ (p^i_1 - p^i_0) = -F^{as}_{P1} \tag{7}$$

However one could clearly observe that no balancing in relation to the TLs manifolds takes place. For this reason we interchanged the globally defined slope to an average slope of POSs manifolds. As shown in equation (7), p_0^i and p_1^i are start and end points of the load case manifolds i and lc is the number of load cases. This constraint almost always shows a significant reduction of the cross sectional area, although it gets outperformed in specific cases.

5. Exemplary shape- and cross section optimization for multiple load cases of an arch

Due to the dimension-limitation with the used solver and the 'layering-method' (see section 3.), we chose a linear arch structure as demonstration object for this paper. The form-finding setup was as follows: the arch span is 10.0 m, the initial geometry consists of a linear polyline with 21 control points ($P_0 - P_{20}$), therefore every segment is initially 0.5 m long; the minimum thickness of the cross section optimization constraint was set to 0.05 m with a specific weight of 24 kN/m²; we apply 3 asymmetrically placed point loads (F_1, F_2, F_3) to the nodes P_3, P_8 and P_{13}. Loads are assembled to 4 load cases: LC^0 = dead load from cross section (DL), LC^1 = DL + F_1 + F_2, LC^2 = DL + F_2 + F_3 and LC^3 = DL + F_3 + F_1. During the form finding we chose the stiffness parameters (k) to reach a target height of 1.5 m (highest point). Small deviations (>0.1 m) are corrected by scaling, so that cross section areas are better comparable for all examples of cross section minimization constraints.

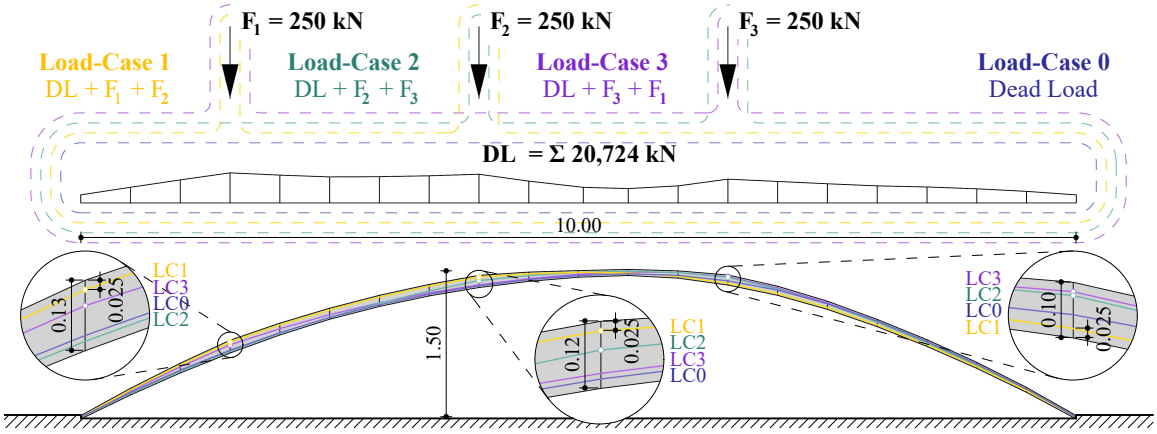

Figure 5: Maximum height constraint, in this case the most efficient strategy to reduce the cross section. Dimensions in meters.

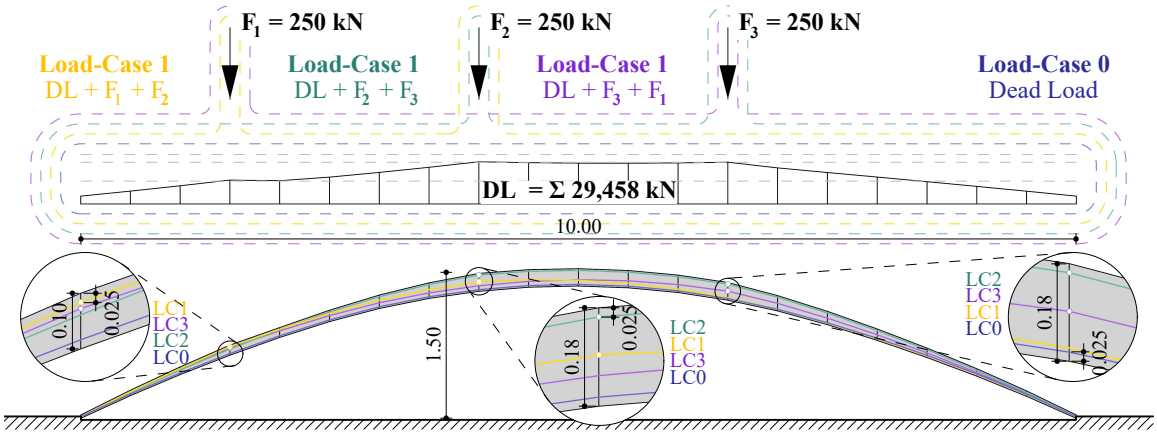

Figure 6: Average height constraint. Dimensions in meters.

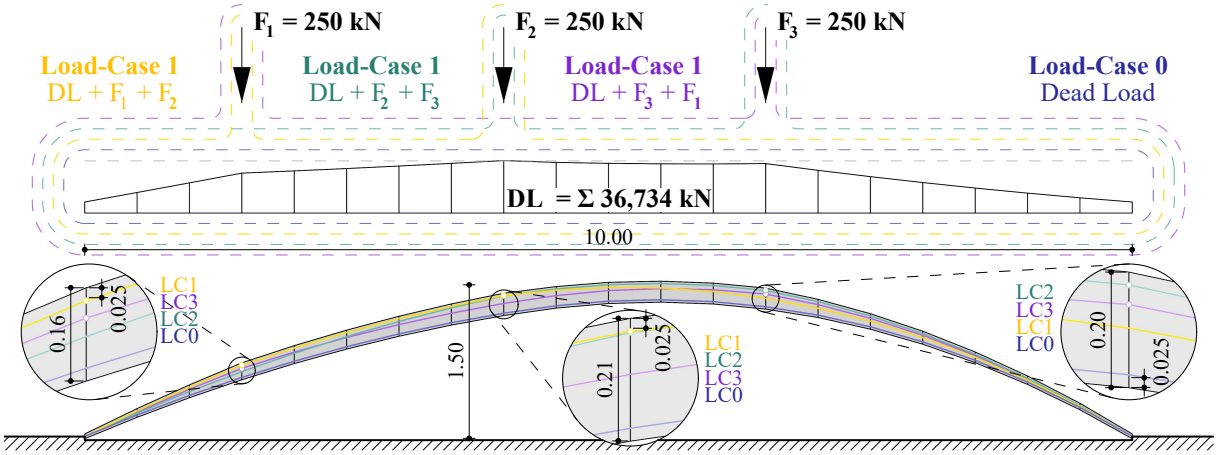

Figure 7: Global slope constraint. Dimensions in meters.

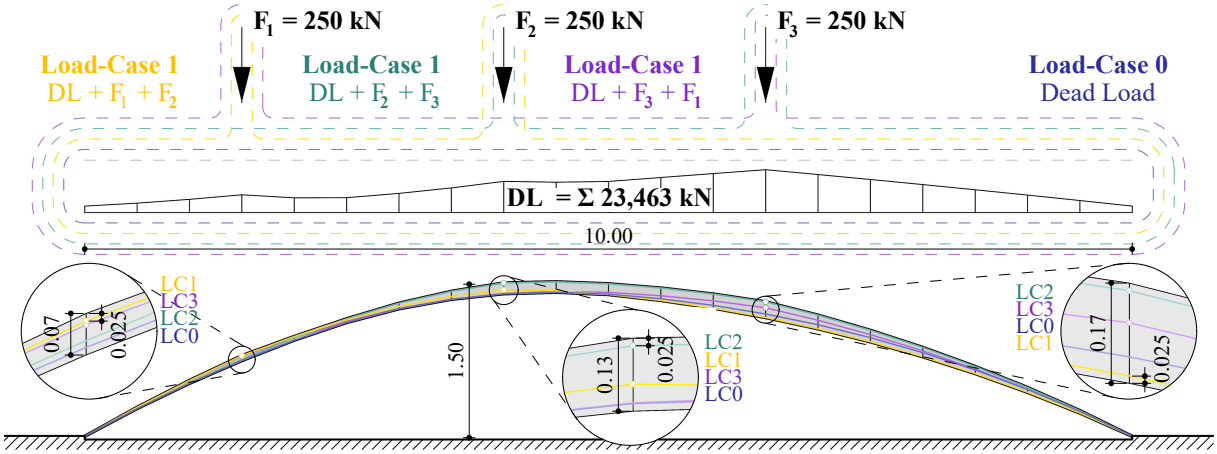

Figure 8: Average slope constraint. Dimensions in meters.

6. Conclusion

The integration of different load cases into the form-finding process is a promising extension for designing efficient shell structures. With the described method and solver, we have successfully conducted form-finding for a compression only arch structure with cross section optimization and variable loads. The initial issues with horizontal displacement were resolved through an alternative formulation of spring elements in the dynamic, particle-based calculation. This principle was also applied to other constraints. It appears to be a promising approach for a variety of constraints in form-finding and is worthwhile to be examined further. The multitude of different objectives became clearly evident in the computation time during the form-finding process. This might be attributed to the formulation of the individual constraints and the implementation of the solver. The used solver defines all manifolds as separate elements, resulting in multiple executions of the same calculations on element level every iteration. A specific solver or implementation is the desired next step of this project, only then, the method can be tested with three-dimensional problems as their element and constraint count increases significantly.

References

[1] J. Heyman, *The Stone Skeleton: Structural Engineering of Masonry Architecture*. Cambridge University Press, 1995.

[2] S. Adriaenssens, P. Block, D. Veenendaal, and C. Williams, Eds., *Shell structures for architecture: Form finding and optimization*. Routledge, 2014.

[3] D. Veenendaal and P. Block, "An overview and comparison of structural form finding methods for general networks," *International Journal of Solids and Structures*, vol. 49, no. 26, pp. 3741–3753, 2012.

[4] P. Cuvilliers, "The constrained geometry of structures: Optimization methods for inverse form-finding design," Dissertation, Massachusetts Institute of Technology, 2020.

[5] G. Senatore and D. Piker, "Interactive real-time physics," *Computer-Aided Design*, vol. 61, pp. 32–41, 2015.

[6] G. Ramesh and C. S. Krishnamoorthy, "Post-buckling analysis of structures by dynamic relaxation," *International Journal for Numerical Methods in Engineering*, vol. 36, no. 8, pp. 1339–1364, 1993.

[7] M. R. Barnes, "Form-finding and analysis of prestressed nets and membranes," *Computers & Structures*, vol. 30, no. 3, pp. 685–695, 1988.

[8] A. Kilian and O. John, "Particle-spring systems for structural form finding," *Journal of the International Association for Shell and Spatial Structures*, no. 46, 2005.

[9] S. Boyd, P. Neal, C. Eric, Borja Peleato, and Jonathan Eckstein, "Distributed optimization and statistical learning via the alternating direction method of multipliers," *Foundations and Trends® in Machine Learning*, vol. 3, no. 1, pp. 1–122, 2010.

[10] S. Bouaziz, S. Martin, T. Liu, L. Kavan, and M. Pauly, "Projective dynamics: Fusing constraint projections for fast simulation," *ACM Trans. Graph.*, vol. 33, no. 154, 2014.

[11] S. Bouaziz, M. Deuss, Y. Schwartzburg, T. Weise, and M. Pauly, "Shape-up: Shaping discrete geometry with projections," *Computer Graphics Forum*, vol. 31, no. 5, pp. 1657–1667, 2012.

[12] D. Piker, "Kangaroo solver," *Kangaroo Group on Grasshopper Forums*, 2017. [Online]. Available: `http://www.grasshopper3d.com/xn/detail/2985220:Comment:1718553`.

[13] J. Harding and P. Shepherd, "Structural form finding using zero-length springs with dynamic mass," *Proceedings of the IASS Symposium*, 2011.

[14] L. Lacoste, "A simplification in the conditions for the zero-length spring seismograph," *Bulletin of theSeismological Society of America*, vol. 25, no. 2, pp. 176–179, 1935.

[15] P. Block and J. Ochsendorf, "Thrust network analysis: A new methodology for three-dimensional equilibrium," *Journal of the International Association for Shell and Spatial Structures*, vol. 48, no. 3, pp. 167–173, 2007.

[16] M. Ripmann, "Rhinovault 2: Funicular form finding based on the compasframework.," [Online]. Available: `https://blockresearchgroup.gitbook.io/rv2/`.